Advanced power core system for the ARIES-AT power plant

(April 23, 2001)

A. R. Raffray[a,*], L. El-Guebaly[b], S. Malang[c], I. Sviatoslavsky[b], M. S. Tillack[a], X. Wang[a], and the ARIES Team

[a]University of California, San Diego, 460 EBU-II, La Jolla, CA 92093-0417, USA

[b]University of Wisconsin, Fusion Technology Institute, 1500 Engineering Drive, Madison, WI 53706-1687, USA

[c]Forschungszentrum Karlsruhe, Postfach 3640, D-76021 Karlsruhe, Germany

Abstract

The ARIES-AT power core was evolved with the overall objective of achieving high performance while maintaining attractive safety features, credible maintenance and fabrication processes, and reasonable design margins as an indication of reliability. The blanket and divertor designs are based on Pb-17Li as coolant and breeder, and low-activation SiC_f/SiC as structural material. Flowing Pb-17Li in series through the divertor and blanket is appealing since it simplifies the coolant routing and minimize the number of cooling systems. However, Pb-17Li provides marginal heat transfer performance in particular in the presence of MHD effects and the divertor design had to be adapted to accommodate the peak design heat flux of 5 MW/m^2. The blanket flow scheme enables operating Pb-17Li at a high outlet temperature (about 1100°C) for high power cycle efficiency while maintaining SiC_f/SiC at a substantially lower temperature consistent with allowable limits. Waste minimization and additional cost savings are achieved by radially subdividing the blanket into two zones: a replaceable first zone and a life of plant second zone. Maintenance methods have been investigated which allow for end-of-life replacement of individual components. This paper summarizes the results of the design study of the ARIES-AT power core focusing on the blanket and divertor and including a discussion of the key parameters influencing the design, such as the SiC_f/SiC properties and the MHD effects, and a description of the design configuration, analysis results and reference operating parameters.

[*] Corresponding author. Tel: 1-858-534-9720; fax: 1-858-534-7716; e-mail: raffray@fusion.ucsd.edu

1. Introduction

The ARIES-AT power plant was evolved to assess and highlight the benefit of advanced technologies and of new physics understanding & modeling capabilities on the performance of advanced tokamak power plants [1]. The design builds on over a decade of experience and effort by the ARIES team in advanced power plant design [e.g. 2,3] and reflects the overall benefit from high-β operation, high temperature superconducting magnet, high power cycle efficiency, and low-cost advanced manufacturing techniques. Figure 1 shows the ARIES-AT power core and Table 1 summarizes the typical geometry and power parameters of the device, emerging from the parametric system studies [4].

The ARIES-AT power core have been developed with the overall objective of achieving high performance while maintaining attractive safety features, credible maintenance and fabrication processes, and reasonable design margins as an indication of reliability. The design utilizes Pb-17Li as breeder and coolant and low-activation SiC_f/SiC composite as structural material. The Pb-17Li operating temperature is optimized to provide high power cycle efficiency while maintaining the SiC_f/SiC temperature under reasonable limits.

2. Power Cycle

The Brayton cycle offers the best near-term possibility of power conversion with high efficiency and is chosen to maximize the potential gain from high temperature operation of the Pb-17Li which after exiting the blanket is routed through a heat exchanger with the cycle He as secondary fluid [5]. The Brayton cycle considered is shown in Figure 2. It includes three-stage compression with two intercoolers and a high efficiency recuperator. Its main parameters are set under the assumption of state of the art components and/or with modest and reasonable extrapolation and are as follows:

- Lowest He temperature in the cycle (heat sink) = 35 °C
- Turbine efficiency = 93%
- Compressor efficiency = 90%
- Recuperator effectiveness = 96%
- He fractional pressure drop in out-of-vessel cycle = 0.025 (this would probably require a He pressure of about 15-20 MPa)

The compression ratio is set to optimize the cycle efficiency while maintaining a reasonable He temperature level at the heat exchanger inlet (which in turn sets the power core Pb-17Li inlet temperature). As illustrated in Figure 3, for a maximum cycle He temperature of 1050°C, a cycle efficiency of 58.5% can be achieved for a compression ratio of 3 [5]. The corresponding He temperature at the heat exchanger inlet is 604°C resulting in a power core Pb-17Li inlet temperature of 654°C under the assumption of a heat exchanger effectiveness of 0.9 and a ratio of Pb-17Li to He thermal capacities of 1.

3. Material Considerations

3.1 SiC_f/SiC

Use of SiC_f/SiC as a structural material is attractive since it enables operation at high temperature and its low decay heat facilitates the accommodation of loss-of-coolant (LOCA) and loss-of-flow (LOFA) events. However, there are some key issues influencing its attractiveness, including: thermal conductivity; parameters limiting the temperature of operation, such as swelling under irradiation and compatibility with the liquid metal; maximum allowable stress limits; lifetime parameters; and fabrication and joining procedures. These issues were addressed in detail in presentations and discussions at the January 2000 International Town Meeting on SiC_f/SiC Design and Material Issues for Fusion Systems [6]vand in a related publication [7]. The SiC_f/SiC parameters and properties used in the ARIES-AT analysis are consistent with the suggestion from this meeting. They are summarized in Table 2 and are briefly commented on below:

3.1.1 Thermal Conductivity

Measurement of transverse thermal conductivity of unirradiated SiC_f/SiC composite tends to fall in the 10-20 W/m-K range for the earlier low-quality SiC fibers. It is expected that the thermal conductivity will be improved as better stoichiometry is achieved in SiC_f/SiC. Recently, measurement of the transverse thermal conductivity of MER CVR SiC/SiC samples yielded 75 W/m-K at room temperature and ≈35 W/m-K at 1000°C. Although there are no confirmed irradiation data on SiC_f/SiC conductivity, it can be assumed that the degradation would be comparable to or less than (on a percentage basis) that observed in pure SiC. Starting with an unirradiated thermal conductivity close to the MER value, it seems reasonable to expect a transverse conductivity of about 15 and possibly up to 20 W/m-K for irradiated material at 1000°C in future generations of SiC_f/SiC.

3.1.2 Stress Limits

It seems clear that conventional stress limits cannot be directly applied to ceramic composites. The non-isotropic behavior of SiC_f/SiC as well as the non-linearity arising from the unique damage mechanisms must be taken into account by sophisticated analyses. In the absence of tools enabling such sophisticated analyses, it is suggested that designers using conventional FEM analysis limit the total combined stress in plane to ≈190 MPa as a conservative first order approximation [7].

3.1.3 Temperature Limits

The maximum SiC_f/SiC temperature limit is set to avoid the void swelling regime. It is not clear at exactly what temperature the transition from point defect swelling to void swelling occurs but from the few existing results, this transition temperature is ≈1000°C.

The maximum interface temperature limit for SiC_f/SiC in contact with Pb-17Li is also not known. Only one data point exists in the open literature on the chemical compatibility of SiC with Pb-17Li at high temperature. From an experiment performed at ISPRA, no compatibility problem was reported for SiC exposed over 1500 hours to static LiPb at 800°C. However, some questions exist regarding the quality and impurity level of the SiC used in these tests. This is certainly an area where R&D is needed. In anticipation of such data, it seems reasonable not to prejudge the blanket limitations and to assume a maximum temperature limit in the blanket zone set by irradiation-induced dimensional changes (≈1000°C). In the future, as new compatibility data become available, this limit can be revised.

3.1.4 Lifetime Limiting Factor

SiC_f/SiC lifetime is one parameter that is particularly hard to characterize based on the limited data and understanding and for which no clear suggestion emerged from the town meeting [6]. However, it is an important parameter affecting the lifetime and replacement cost of in-vessel component and needs to be characterized for power plant studies. Here, consistent with previous ARIES studies [2], a 3% burnup limit is assumed (corresponding to a neutron fluence of 18 MW-a/m^2), subject to R&D verification of impact of He and H production on thermomechanical properties of SiC_f/SiC.

3.2 Pb-17Li and W Properties

Temperature-dependent properties of Pb-17Li were used in the analysis. However, the expressions for these properties, as shown for example in Ref. [8], tend to be limited to rather low ranges of temperature, at most about 700°C. In the absence of R&D data it was decided to extrapolate from this property data base and to strongly recommend as future R&D an effort to measure Pb-17Li properties at high temperature. The final design would have to be re-optimized if Pb-17Li properties (in particular the thermal conductivity) at high temperatures were found to be substantially different from the extrapolated values.

Table 3 shows the typical Pb-17Li properties estimated for an average temperature of 850°C. The W properties used in the divertor analysis are also shown in the table.

4. Blanket and Coolant Configuration

For waste minimization and cost saving reasons, the blanket is subdivided radially into two zones, as shown in Figure 1: a replaceable first zone in the inboard and outboard, and a life of plant second zone in the outboard. To simplify the cooling system and minimize the number of coolants, the Pb-17Li is used to cool the blanket as well as the divertor and hot shield regions. The coolant is fed through an annular ring header surrounding the power core from which it is routed to each of 16 reactor sectors through the following five sub-circuits:

(1) series flow through the lower divertor and inboard blanket region (see Figure 4; total thermal power and mass flow rate = 501 MW and 6100 kg/s);

(2) series flow through the upper divertor and one segment of the first outer blanket region (see Figure 5; total thermal power and mass flow rate = 598 MW and 7270 kg/s);

(3) flow through the second segment of the first outer blanket region (see Figure 6; total thermal power and mass flow rate = 450 MW and 5470 kg/s);

(4) series flow through the inboard hot shield region and first segment of the second outer blanket region (see Figure 7; total thermal power and mass flow rate = 182 MW and 4270 kg/s); and

(5) series flow through the outboard hot shield region and second segment of the second outer blanket region (see Figure 8; total thermal power and mass flow rate = 140 MW and 1700 kg/s).

As illustrated in Figures 9 and 10, the blanket design is modular and consists of a simple annular box through which the Pb-17Li flows in two poloidal passes. Positioning ribs are attached to the inner annular wall forming a free floating assembly inside the outer wall. These ribs divide the annular region into a number of channels through which the coolant first flows at high-velocity to keep the outer walls cooled. The coolant then makes a U-turn and flows very slowly as a second pass through the large inner channel from which the Pb-17Li exits at high temperature. This flow scheme enables operating Pb-17Li at a high outlet temperature (1100°C) while maintaining the blanket SiC_f/SiC composite and SiC/PbLi interface at a lower temperature (~1000°C). The first wall consists of a 4-mm SiC_f/SiC structural wall on which a 1-mm CVD SiC armor layer is deposited.

5. Blanket Analysis

Detailed 3-D neutronics analyses of the power core were performed yielding a tritium breeding ratio of 1.1 and the energy multiplication and wall loading values shown in Table 1 [9]. The volumetric heat generation profiles from these analyses were used in subsequent thermal investigations. Of the three blanket regions, the first outboard region is subjected to the highest heat loads. A typical module in an outboard segment cooled in series with the upper divertor was the focus of the thermal analyses which are described below and whose results are summarized in Table 4.

For these analyses, the plasma heat flux profile was estimated by considering bremstrahlung radiation, line radiation and synchotron radiation with average and peak values of 0.26 MW/m^2 and 0.34 MW/m^2, respectively [4]. The analysis assumes no radiation to the first wall from the 256 MW transport power to the divertor. The design can be re-optimized if such radiation becomes appreciable under future physics scenarios.

5.1 Thermal-Hydraulic Analysis

Even though the SiC_f/SiC provides insulated walls thereby minimizing MHD effects, the analysis conservatively assumes MHD-laminarized flow of the Pb-17Li in the blanket and heat transfer by conduction only. This is also justified by the observation that the MHD Re for the transition to turbulent flow estimated from the given Hartmann number, H (~500H for a transverse magnetic field[10]) is higher than the actual flow Re, as shown in Table 3. The temperature profile through the blanket was estimated by a moving coordinate analysis which follows the Pb-17Li flow through the first-pass annular wall channel and then through the second-pass large inner channel. In general, MHD effects would tend to flatten the velocity profile and, for simplicity, the analysis assumed slug flow in both channels. The annular wall rib spacing is used as MHD flow control to achieve a higher flow rate through the first wall (with larger toroidal spacing) than through the side and back walls. For example, having three channels in the module first wall and thirteen in the back wall allows for a high velocity of 4.2 m/s in the first wall channels and a lower velocity of 0.66 m/s in the back wall channel for the same MHD pressure drop. The second poloidal pass of the Pb-17Li through the large inner channel is much slower with an average velocity of 0.11 m/s.

Figure 11 illustrates the results for a typical outboard module. Even though the average outlet Pb-17Li temperature is 1100°C, this design results in a maximum SiC temperature at the first wall (radial distance = 0) of 1009°C, a maximum SiC_f/SiC temperature of 996°C. and a maximum blanket SiC/Pb-17Li interface temperature at the inner channel wall of 994°C, which satisfy the maximum temperature limits shown in Table 2.

The first wall and blanket pressure drops were estimated as a function of the Hartmann number, H, and wall to fluid conductance ratio, C, based on the following expression for the pressure gradient under MHD effects, $\frac{dP}{dx}$ [10]:

$$\frac{dP}{dx} = \frac{\mu v}{a}\left(\frac{H^2 \tanh H}{H - \tanh H} + \frac{H^2 C}{1 + C} - 3 + \frac{dP'}{dx'}\right) \quad (1)$$

$$C = \frac{\sigma_w t_w}{\sigma_L a} \quad (2)$$

$$H = aB\sqrt{\frac{\sigma_L}{\mu}} \quad (3)$$

where μ is the liquid viscosity; v the liquid average velocity; a the channel half-width in the direction parallel to the magnetic field, B; $\frac{dP'}{dx'}$ is the ordinary laminar-flow pressure drop (=7.11 for square channels); σ_w the wall electrical conductivity; σ_L the liquid electrical conductivity; and t_w the wall thickness.

The resulting overall blanket pressure drop is about 0.25 MPa.

5.2 Stress Analysis

Stress analyses were performed both on the module outer and inner shells. A 1-MPa inlet pressure is assumed for the coolant which adequately accounts for both the pressure drop through the blanket (~0.25 MPa) and the hydrostatic pressure due to the ~6 m Pb-17Li

(~0.5 MPa) column. The outer wall is designed to withstand this pressure while the inner wall is designed to withstand the difference between blanket inlet and outlet pressures (0.25 MPa). There are six modules per outboard segment as shown in Figure 9. These modules are brazed to one another and the side walls of all the inner modules are pressure balanced. However, the side walls of the outer modules must be reinforced to accommodate the 1 MPa coolant pressure. For example, Figure 12 shows that the maximum side wall pressure stress is 85 MPa for a 2-cm thick side wall. The side wall can be tapered radially and poloidally by tailoring the thickness to maintain a uniform stress. This would reduce the SiC volume fraction and benefit tritium breeding. In addition, the thermal stress at this location is small and the sum of the pressure and thermal stresses is well within the 190 MPa limit. This margin can be considered as a measure of reliability and provides some flexibility if the final blanket design optimization shows that further reductions of the SiC volume fraction are needed for better tritium breeding.

From Figure 12, the pressure stress at the first wall is quite low, ~60 MPa. The corresponding thermal stress is also very reasonable and the design provides substantial margin in this regard being able to accommodate more than twice the reference heat flux values. For example, Figure 13 shows the 3-D thermal stress distribution in the module for a case assuming a simple linear heat flux poloidal distribution (with average and maximum values of 0.6 and 0.7 MW/m^2, respectively) and an effective heat transfer coefficient of 15,000 W/m^2-K in the Pb-17Li channel. The maximum thermal stress in this case is 114 MPa resulting in a modest combined stress of 174 MPa still well within the 190 MPa limit.

Figure 14 shows the pressure stress in an inner module wall of 8-mm side thickness. The thickness of the upper and lower wall is 5 mm. The maximum stress is 116 MPa again well within the maximum allowable stress. In addition, the maximum pressure differential of ~0.25 MPa occurs at the lower poloidal location. The inner wall thickness could be tapered down to ~5 mm at the upper poloidal location if needed to minimize the SiC volume fraction.

The design has been optimized to the given dimensions to provide reasonable margins on stress limits. As mentioned above, it also provides the possibility of reducing the SiC volume fraction for improved tritium breeding by tapering the side wall thickness for both inner and outer shells. If further improvement in the tritium breeding is required, the blanket thickness can also be adjusted. For example, the second outboard blanket region could be increased by ~10 cm. However, the side wall thicknesses of the outer module in each segment and of the inner shell in each module would have to be adjusted accordingly to meet the stress limits.

5.3 Safety Analysis

The activation, decay heat, and waste disposal analyses performed in support of the ARIES-AT design are described in Refs. [11,12]. The decay heat results were used to perform 2-D safety analyses of the power core which showed that the low decay heat of SiC enables accommodation of any loss-of-coolant (LOCA) or loss-of-flow (LOFA) scenarios without serious consequences to the blanket structure [12,13]. Interestingly, because of the low decay heat of SiC as compared to Pb-17Li, the analyses showed that the resulting maximum power core temperature was about 50°C higher in the case of a LOFA than in the case of a LOCA, but still well within the limits.

6. Divertor Configuration

Pb-17Li has a relatively low thermal conductivity and tends to offer limited heat removal performance in particular in the presence of a magnetic field. In order to accommodate MHD effects, the proposed design:

- Minimizes the interaction parameter (<1) which represents the ratio of MHD to inertial forces;

- Directs the flow in the high heat flux region parallel to the toroidal magnetic field; and
- Minimizes the Pb-17Li flow path and residence time in the high heat flux region.

The design is illustrated in Figure 15, which shows a cross-section of a divertor plate. It consists of a number of 2-cm x 2.5-cm SiC_f/SiC poloidal channels. The front SiC_f/SiC wall is very thin (0.5 mm) in order to maintain the maximum temperature and combined stress limits to ≤1000°C, and ≤190 MPa, respectively. A 3.5-mm plasma facing layer of sputter-resistant W alloy (with 0.2 wt% TiC) is bonded to the thin SiC_f/SiC to provide additional structure to accommodate the 1.8-MPa Pb-17Li pressure and to provide sacrificial armor (≈1mm). In this design, as in previous ARIES studies, the philosophy is to operate with a ~10% margin within the plasma β limit to avoid disruptions, which is also consistent with the understanding that a utility company is not likely to buy or operate a power plant with frequent disruptions. However, the design should be able to handle a few rare disruptions without loss of investment and the ≈1-mm sacrificial W armor is provided for this purpose.

In each channel a T-shaped flow separator is inserted. The Pb-17Li flows poloidally through one half of the channel which acts as an inlet header. The flow is then forced to the PFC region through small holes at one side of the channel. The flow through these small holes is inertial with an interaction parameter <1. The Pb-17Li then flows toroidally to cool the high heat flux region through a very short flow path (2 cm). It is then routed back to the other side of the poloidal channel serving as outlet header. The Pb-17Li velocity through the toroidal PFC channel can be adjusted by changing the dimension of this channel or by increasing the number of toroidal passes through a plate. The reference design uses a 2-mm thick channel and 2-pass flow resulting in toroidal channel velocities and residence times of about 0.4 m/s and 0.05 s, respectively

7. Divertor Analysis

The average heat flux on the divertor is 1.75 MW/m^2 and, in analogy with the analysis shown in Ref. [3], a corresponding peak heat flux of 5 MW/m^2 is assumed for the analysis. The heat transfer performance is slightly more challenging for the lower divertor than for the upper divertor since the former is part of a Pb-17Li circuit with a somewhat lower mass flow rate (see Section 4) than the latter. Consequently, the divertor analyses described below are focused mostly on the lower divertor. However, some key parameters for the upper divertor are also included in the overall summary of divertor design parameters shown in Table 5. The parameters for the inner and outer divertor plates are also shown separately when there are significant differences. This was found not to be the case for the maximum material temperature calculations, for example, as the effect of the higher Pb-17Li temperature in the inner divertor (the Pb-17Li flows in series through the outer and then inner divertor plates) is compensated by the effect of higher Pb-17Li velocity resulting from the geometry and lower number of tubes in the inner divertor region.

7.1 Thermal-Hydraulic Analysis

The 2-D moving coordinate method was used for the flow analysis under the assumption of MHD-laminarized slug flow in the toroidal channel. Figure 16 shows the typical results for an upper divertor case with an inlet Pb-17Li temperature of 653°C, a W thickness of 3 mm, a SiC_f/SiC first wall thickness of 0.5 mm, a Pb-17Li toroidal channel thickness of 2 mm, a SiC_f/SiC inner wall thickness of 0.5 mm, a Pb-17Li velocity of 0.35 m/s and a surface heat flux of 5 MW/m^2. The maximum W temperature is ≈1150°C, and the maximum SiC_f/SiC temperature is ≈950°C. The lowest W temperature is ≈800°C for this case and will be about 700-800°C for lower local heat fluxes. This is somewhat lower than the expected value to avoid severe irradiation embrittlement based on the scarce data available[14]. However, a margin of about 50°C exists for the SiC_f/SiC maximum temperature and, as new R&D data on W mechanical properties under irradiation become available, the design and coolant conditions can be reoptimized to increase the minimum W operating temperature.

The resulting Pb-17Li MHD pressure drop through the divertor for the proposed flow configuration is estimated from Eqs. (1) to (3) to be about 0.7 MPa. This is significantly larger than the blanket pressure drop. To minimize pressure stresses in the piping and blanket system, the Pb-17Li in the inlet manifold is kept at 1.1 MPa. The Pb-17Li is then pressurized to 1.8 MPa just before flowing though the divertor by means of an E-M pump making use of the existing toroidal magnetic field. The outlet flow from the divertor then rejoins the blanket inlet manifold at about 1.1 MPa.

7.2 Stress Analysis

Stress analyses were performed to size the divertor. For example, the thermal stress distribution is shown in Figure 17 for a surface heat flux of 5 MW/m^2. From the figure, the maximum thermal stress at the plasma-facing wall is low in the W (≈45 MPa) but is of more concern in the SiC_f/SiC (165 MPa). However, the corresponding pressure stress in the SiC_f/SiC also calculated from ANSYS is modest (25 MPa for an inner Pb-17Li pressure of 1.8 MPa). The resulting combined stress is 190 MPa which satisfies the maximum allowable stress criterion for SiC_f/SiC.

8. Fabrication and Maintenance

As a reliability measure, minimization of the number and length of brazes was a major factor in evolving the fabrication procedures for the blanket and divertor. For the blanket, the proposed fabrication scheme requires three radial/toroidal coolant-containment brazes per module, as illustrated by the following fabrication steps for an outboard segment consisting of 6 modules (see Figures 18(a), (b), (c), and (d)):

1. Manufacturing separate halves of the SiC_f/SiC poloidal module by SiC_f weaving and SiC Chemical Vapor Infiltration (CVI) or polymer process;
2. Inserting the free-floating inner separation wall in each half module;
3. Brazing the two half modules together at the midplane;
4. Brazing the module end cap;
5. Forming a segment by brazing six modules together (this is a joint which is not in contact with the coolant); and
6. Brazing the annular manifold connections to one end of the segment.

The divertor fabrication scheme also aims at minimizing brazing and can be summarized as follows (see Figure 19):

1. Manufacture separate SiC_f/SiC toroidal halves of the divertor plate by SiC_f weaving and SiC CVI or polymer process; maintain constant channel toroidal dimensions but tapered side wall thicknesses to account for torus geometry;
2. Insert the inner SiC_f/SiC separation wall in each divertor channel;
3. Braze the two toroidal halves of the divertor plate together;
4. Braze the end cap and manifold on each end; and
5. Bond theW layer to the SiC_f/SiC front wall by plasma spray.

Maintenance methods have been investigated which allow for end-of-life replacement of individual components. These are discussed in detail in Ref [15].

9. Manifold

An annular Pb-17Li coolant manifold is used to feed the divertor and blanket, with the lower temperature inlet flow in the outer channel and the higher temperature outlet flow in the inner channel. In this way any effect of the high SiC/Pb-17Li interface temperature on the manifold inner wall would only result in a leak to the manifold outer channel, which would not be of major consequence. However, the structural integrity of the configuration would be ensured by the low temperature outer channel.

One issue relates to the difficulty of maintaining the maximum SiC/Pb-17Li interface temperature at the outlet side of the manifold well below the Pb-17Li outlet temperaure (1100°C). This can only be done by maintaining a heat flux between the outlet and inlet flow to provide a temperature gradient at the outlet wall such that the wall interface temperature would be lower than the outlet Pb-17Li temperature. This could be achieved to some extent by adjusting the annular manifold geometry (affecting the velocity and heat transfer coefficient in the inner and outer channels) and inner wall thermal conductivity. Figure 20 illustrates this effect for a manifold servicing the outboard blanket segment from the ring header. For example, the maximum Pb-17Li/SiC interface temperature can be reduced to about 1000°C for manifold inner and outer radii of 0.05 m and 0.12 m and an inner wall thermal conductivity of 10 W/m-K. However, the corresponding heat flux from the hot outlet Pb-17Li to the cold inlet Pb-17Li results in a bulk temperature increase of the inlet flow of more than 100°C which negates the initial effect.

All manifold flows are in regions with very low or no radiation and with the higher temperature outlet flow in the inner channel such that the structural integrity of the configuration depends mostly on the low temperature outer channel wall. Thus, it seems reasonable to accept a maximum Pb-17Li/SiC interface temperature in the manifold comparable to the outlet Pb-17Li temperature and to set the manifold annular dimensions so as to minimize the heat flux between the hot and cold legs while maintaining a reasonable pressure drop (see Figure 21). As data become available on unirradiated Pb-17Li/SiC compatibility at high temperature, this approach could be revised. For the above case, this would correspond to manifold inner and outer radii of ~0.06 m and 0.12 m and an inner wall thermal conductivity of 1 W/m-K.

Tritium has a high vapor pressure over Pb-17Li and operation of SiC_f/SiC at high temperature raises the question of whether tritium permeation and inventory would be an issue. For the annular manifold, tritium permeation is less of a concern since some level of permeation through the high temperature SiC_f/SiC inner channel wall would be allowable as long as the corresponding tritium inventory is acceptably low and permeation through the colder outer channel wall is acceptably low. Of more concern would be the potential permeation in the heat exchanger between the Pb-17Li primary side and the He secondary side. SiC_f/SiC would be a logical candidate as heat exchanger material although no detailed design of the heat exchanger has been performed and no final decision on the heat exchanger material made. Ref. [16] includes a review of tritium solubility and diffusivity in SiC, highlighting the experimental difficulties encountered in attempting to absorb hydrogen isotopes into the bulk of the ß-SiC even at temperatures as high as 1000°C. This suggests that tritium retention in the SiC_f/SiC walls of the power core channels should be small. It also suggests that tritium permeation in the heat exchanger should not be a major issue in particular if a coating of fully-dense ß-SiC (such as by CVD) is present, as is proposed for the current design.

10. Conclusions

The ARIES-AT power core utilizes high temperature Pb-17Li as breeder and coolant and low-activation SiC_f/SiC composite as structural material. High power cycle efficiency (~58.5%) is achieved while the in-reactor material limits are accommodated by the design. Both the blanket and divertor designs are based on a simple geometry. Credible fabrication procedures have been evolved which minimize the coolant containing joints and enhances reliability. The design process strives as much as to maintain comfortable stress limit margins as an additional reliability measure.

Key issues requiring R&D attention are mostly linked with the SiC_f/SiC material. They include development of low-cost high-quality material and joining methods and characterization of key SiC_f/SiC properties and parameters at high temperature and under irradiation, in particular thermal conductivity, temperature limits (based on strength degradation, compatibility with Pb-17Li, and He swelling), and lifetime. In addition, Pb-17Li properties at high temperature need to be measured.

Acknowledgement

This work was supported by U.S. Department of Energy under Contract DE-FC03-95ER54299

References

1. F. Najmabadi, et al., and the ARIES Team, Overview of the ARIES-AT advanced tokamak, advanced technology power plant study, Fus. Eng. & Des., this issue.

2. F. Najmabadi, R. Conn, et al., The ARIES-I tokamak reactor study, Final report, UCLA-PPG-1323, UCLA, CA, 1991.

3. F. Najmabadi and the ARIES Team, Overview of the ARIES-RS reversed-shear tokamak power plant study, Fus. Eng. & Des., 38 (1997) 3-25,.

4. R. L. Miller, et al., System studies in support of ARIES-AT, Fus. Eng. & Des., this issue.

5. R. Schleicher, A. R. Raffray, C. P. Wong, An assessment of the Brayton Cycle for high performance power plant, Proc. 14th ANS Topical Meeting on Fusion Energy, Park City, USA, October 2000, to appear.

6. International town meeting on SiC/SiC design and material issues for fusion systems, Oak Ridge National Laboratory, January 18-19, 2000, http://aries.ucsd.edu/PUBLIC/SiCSiC/

7. A. R. Raffray, M. Billone, R. H. Jones, et al., Design and material issues for high performance SiC_f/SiC-based fusion power cores, Fus. Eng. & Des., to appear.

8. Property data base from ARIES web site, http://ashley.ucsd.edu/PROPERTIES/lipb.html

9. L. A. El-Guebaly, et al., and the ARIES Team, Nuclear performance assessment for ARIES-AT, Fus. Eng. & Des., this issue.

10. M. A. Hoffman and G. A. Carlson, Magnetic field effects in fusion reactor blankets, Proceedings of the 13th Intersociety Energy Conversion Energy Conference, SAE P-75, IEEE 78-CH1372, San Diego, August 20-25, 1978.

11. D. Henderson, L. El-Guebaly, A. Abdou, P. Wilson, and The ARIES Team, Activation, decay heat, and waste disposal analyses for ARIES-AT power plant, Proc. 14th ANS Topical Meeting on Fusion Energy, Park City, USA, October 2000, to appear.

12. D. Petti, et al., and the ARIES Team, ARIES-AT safety design and analysis, Fus. Eng. & Des., this issue.

13. E. Mogahed, L. El-Guebaly, A. Abdou, P. Wilson, D. Henderson, and the ARIES Team, Loss of coolant and loss of flow accident analyses for ARIES-AT power plant,

Proc. 14th ANS Topical Meeting on Fusion Energy, Park City, USA, October 2000, to appear.

14. S. J. Zinkle,N. M. Ghoniem, Operating temperature windows for fusion reactor structural materials, Fus. Eng. Des., 51-52 (2000) 55-71.

15. L. Waganer, et al., and the ARIES Team, ARIES-AT configuration and maintenance system definitions and analysis, Fus. Eng. & Des., this issue.

16. M. S. Tillack, et al., “Fusion Power Core Engineering for the ARIES-ST Power Plant,” Fus. Eng. & Des., to appear.

List of Figures

1. ARIES-AT power core (radial dimension in m).

2. Brayton cycle assumed for power conversion

3. Cycle efficiency and He temperature at inlet of heat exchanger as a function of compression ratio for Brayton cycle.

4. Circuit 1 - series flow through the lower divertor and inboard blanket region.

5. Circuit 2 - series flow through the upper divertor and one segment of the first outer blanket region.

6. Circuit 3 - flow through the second segment of the first outer blanket region.

7. Circuit 4 - series flow through the inboard hot shield region and first segment of the second outer blanket region.

8. Circuit 5 - series flow through the outboard hot shield region and second segment of the second outer blanket region.

9. Cross-section of ARIES-AT outboard blanket segment (radial dimension in m).

10. Cross-section of ARIES-AT outboard blanket module (all dimensions in cm).

11. Temperature distribution through outboard blanket module.

12. Pressure stress distribution in blanket module outer wall.

13. Thermal stress distribution in toroidal half of blanket module.

14. Pressure stress distribution in blanket module inner wall.

15. Cross-section of divertor plate (all dimensions in cm).

16. Temperature distribution through plasma-facing region of outer divertor plate.

17. Thermal stress distribution in divertor plate.

18(a), (b), (c), (d) Step-wise blanket fabrication procedure

19. Assembled divertor plate segment

20. Maximum Pb-17Li/SiC interface temperature in manifold and corresponding Pb-17Li temperature as a function of annular manifold inner radius for one of 16 manifolds feeding an outboard blanket segment from the ring header (Pb-17Li mass flow rate = 45.4 kg/s; Pb-17Li inlet/outlet temperatures = 653/1100°C; pipe length = 8 m; outer radius, r_o, = 0.12 m; SiC_f/SiC outer and inner wall thickness = 5 mm). Cases with assumed SiC_f/SiC inner wall conductivies of 1 and 10 W/m-K are shown.

21. Total manifold pressure drop as a function of annular manifold inner radius for fixed outer radius, length and flow rate (see Figure 20; entry/exit loss coefficient = 2).

List of Tables

Table 1 Typical ARIES-AT Machine and Power Parameters

Machine Geometry	
Major Radius	5.2 m
Minor Radius	1.3 m
Outboard FW Location at Midplane	6.5 m
Outboard FW Location at Lower/Upper End	4.9 m
Inboard FW Location	3.9 m
On-Axis Magnetic Field	5.9 T
Toroidal Magnetic Field at Inboard FW	7.9 T
Toroidal Magnetic Field at Outboard FW	4.7 T
Toroidal Magnetic Field at Divertor (Outer/Inner)	7/7.9 T
Power Parameters	
Fusion Power	1719 MW
Neutron Power	1375 MW
Alpha Power	344 MW
Current Drive Power	25 MW
Transport Power to the Divertor	256 MW
Blanket Multiplication Factor	1.1
Maximum Thermal Power	1897 MW
Average Neutron Wall Load	3.2 MW/m^2
Outboard Maximum Wall Load	4.8 MW/m^2
Inboard Maximum Wall Load	3.1 MW/m^2

Table 2 SiC_f/SiC properties and parameters assumed in this study [6]

Density	~3200 kg/m^3
Density Factor	0.95
Young's Modulus	~200-300 GPa
Poisson's ratio	0.16-0.18
Thermal Expansion Coefficient	4x10^{-6} K^{-1}
Thermal Conductivity	~20 W/m-K
Thermal Conductivity through Thickness	~20 W/m-K
Maximum Allowable Combined Stress	~190 MPa
Max. Allowable Operating Temperature	~1000 °C
Max. Allowable SiC/LiPb Interface Temp.	~1000°C
Maximum Allowable SiC Burnup	~3%
Electrical Resistivity	2x10^{-3} ohm-m

Table 3 Typical Pb-17Li properties (at 850°C) and W properties used in this study

Pb-17Li at 850°C	
Density	8560 kg/m^3
Heat Capacity	185 J/kg-K
Thermal Conductivity	24.1 W/m-K
Dynamic Viscosity	6.51x10^{-4} kg/m-s
Prandtl Number	5x10^{-3}
Electrical Resistivity	1.5x10^{-6} ohm-m
Tungsten	
Density	18,950 kg/m^3
Thermal Conductivity	113 W/m-K
Poisson’s Ratio	0.2
Young’s Modulus	370 GPa
Thermal Expansion Coefficient	4.5 x10^{-6} K^{-1}

Table 4 Summary of Typical ARIES-AT Blanket Parameters (as represented by first outboard region)

Overall Geometry	
Inboard Blanket First Wall Area	111 m^2
Outboard Blanket First Wall Area	244 m^2
Total Blanket First Wall Area	355 m^2
Pb-17Li Coolant	
Power Core Inlet Temperature	654°C
Inlet Temp. to Outboard Blanket Region I	764°C
Blanket Outlet Temperature	1100°C
Blanket Inlet Pressure	1 MPa
Blanket Pressure Drop	0.25 MPa
Total Mass Flow Rate	22,700 kg/s
Mass Flow Rate per Module in O/B Blkt Region I	76 kg/s
Outboard Blanket Region I	
Number of Sectors/Segments	16/32
Number of Modules per Outboard Segment	6
Module Poloidal Dimension	6.8 m
Average Module Toroidal Dimension	0.19 m
First Wall SiC_f/SiC Thickness	4 mm
First Wall CVD SiC Thickness	1 mm
First Wall Annular Channel Thickness	4 mm
Average Pb-17Li Velocity in First Wall	4.2 m/s
First Wall Channel Re	3.9×10^5
First Wall Channel Transverse Hartmann Number	4340
MHD Turbulent Transition Re	2.2×10^6
First Wall MHD Pressure Drop	0.19 MPa
Maximum SiC_f/SiC Temperature	996°C
Maximum CVD SiC Temperature	1009 °C
Maximum Pb-17Li/SiC Interface Temperature	994 °C
Average Pb-17Li Velocity in Inner Channel	0.11 m/s

Table 5 Summary of Typical ARIES-AT Divertor Parameters

Divertor Geometry	
Divertor Plate Poloidal Dimension (Outer/Inner)	1.5/1.0 m
Divertor Channel Toroidal Pitch	2.1 cm
Divertor Channel Radial Dimension	3.2 cm
Number of Divertor Channels (Outer/Inner)	1316/1167
Total Number of Divertor Channels (Upper+Lower)	4967
SiC_f/SiC Plasma-Side Thickness	0.5 mm
W Thickness	3.5 mm
Plasma Facing Channel Thickness	2 mm
Number of Toroidal Passes	2
Toroidal Dimension of Inlet and Outlet Feeder Slots	1 mm
Inboard Divertor Plate Area	40.9 m^2
Outboard Divertor Plate Area	54.9 m^2
Divertor Dome Area	50.8 m^2
Total Divertor Area	146.6 m^2
Pb-17Li Coolant and Thermal-Hydraulics	
Divertor Inlet Temperature	654°C
Divertor Outlet Temperature (Upper/Lower)	785/764°C
Divertor Inlet Pressure	1.8 MPa
Divertor Pressure Drop (Lower/Upper)	0.55/0.7 MPa
Circuit Mass Flow Rate (Lower/Upper)	6100/7270 kg/s
Velocity in Lower Divertor PFC Channel (Outer/Inner)	0.35/0.6 m/s
Velocity in Upper Divertor PFC Channel (Outer/Inner)	0.42/0.71 m/s
Velocity in Inlet & Outlet Slot to PFC Channel	0.9-1.8 m/s
Interaction Parameter in Inlet/Outlet Slot	0.46-0.73
Maximum SiC_f/SiC Temperature (Lower/Upper)	970/950°C
Maximum W Temperature (Lower/Upper)	1145/1125°C
W Pressure + Thermal Stress	≈25+45 MPa
SiC_f/SiC Pressure + Thermal Stress	≈25+165 MPa

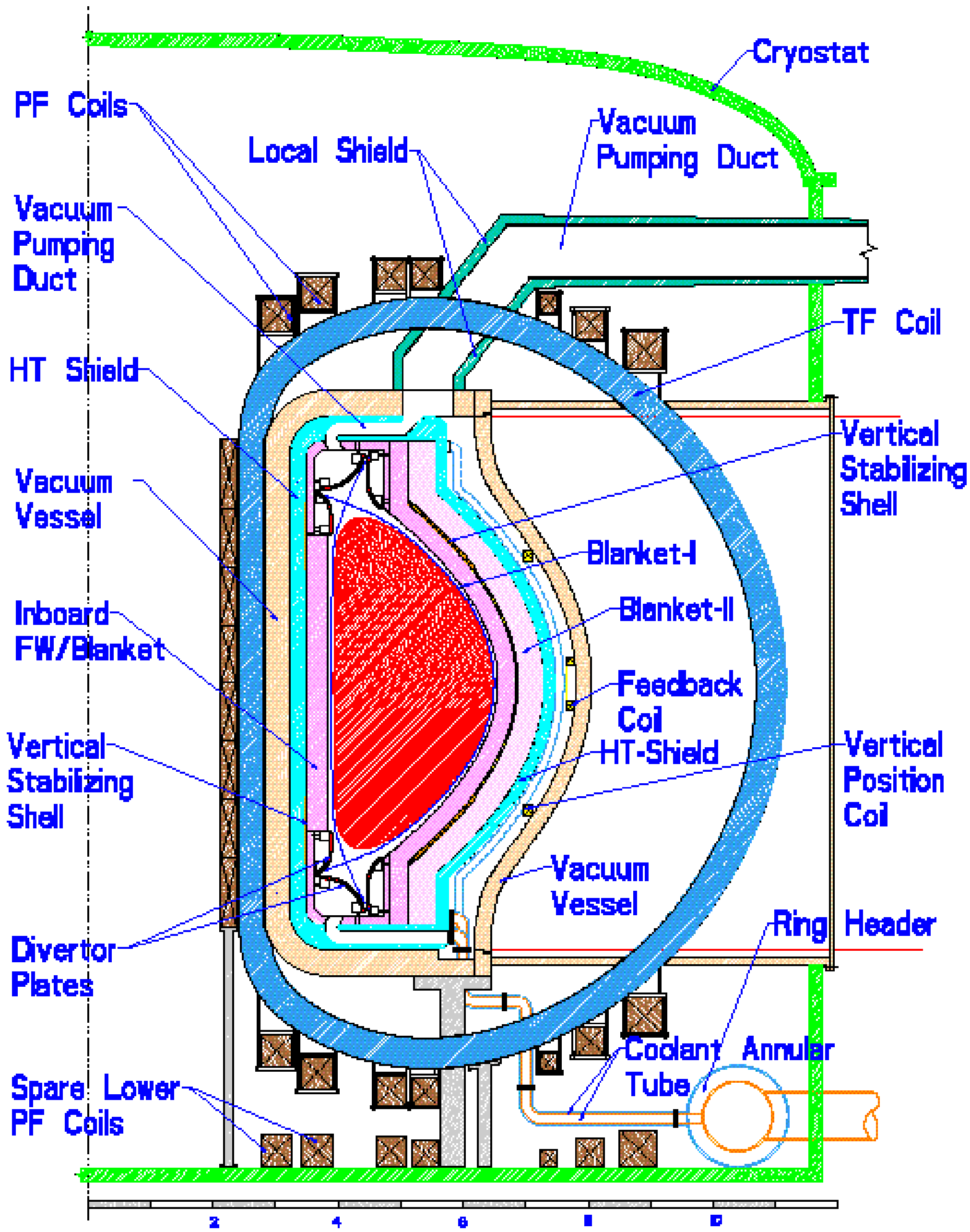
Cryostat
PF Coils
Local Shield
Vacuum Pumping Duct
Vacuum Pumping Duct
TF Coil
HT Shield
Vertical Stabilizing Shell
Vacuum Vessel
Blanket-I
Inboard FW/Blanket
Blanket-II
Feedback Coil
HT-Shield
Vertical Stabilizing Shell
Vertical Position Coil
Vacuum Vessel
Divertor Plates
Ring Header
Coolant Annular Tube
Spare Lower PF Coils
2
4
6
8
10

Figure 1

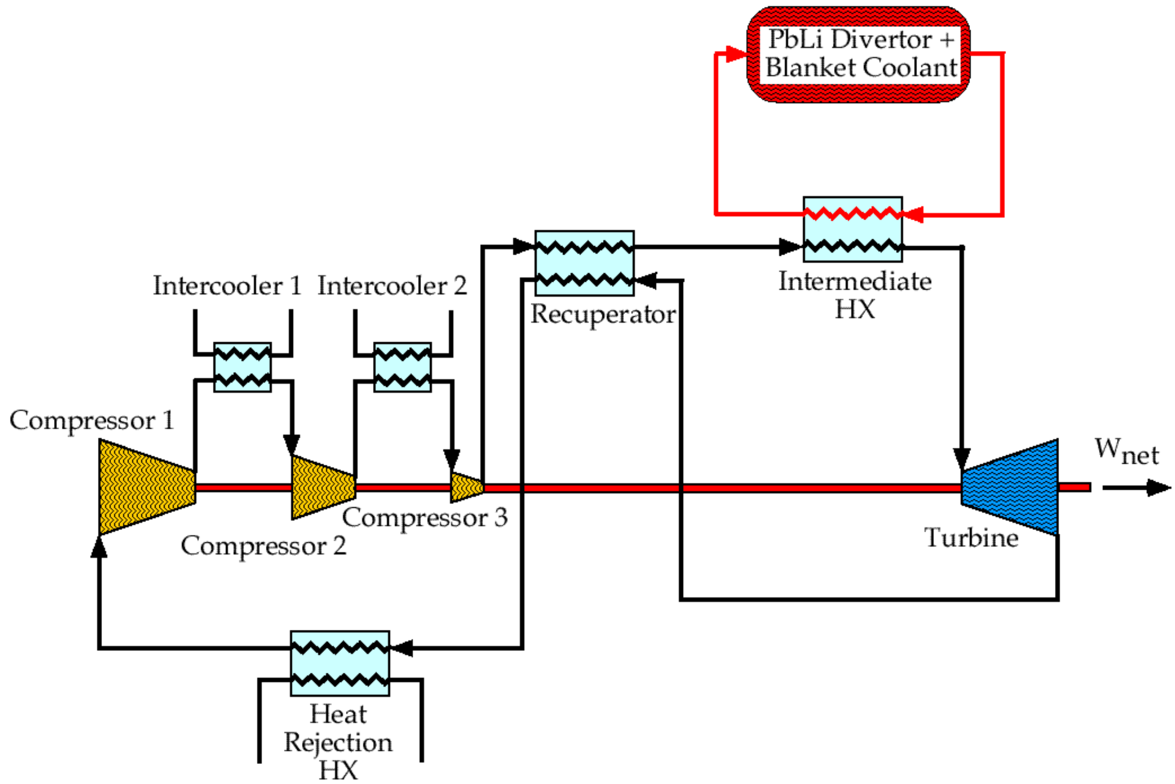

PbLi Divertor +
Blanket Coolant
Intercooler 1
Intercooler 2
Recuperator
Intermediate
HX
Compressor 1
W_{net}
Compressor 3
Compressor 2
Turbine
Heat
Rejection
HX

Figure 2

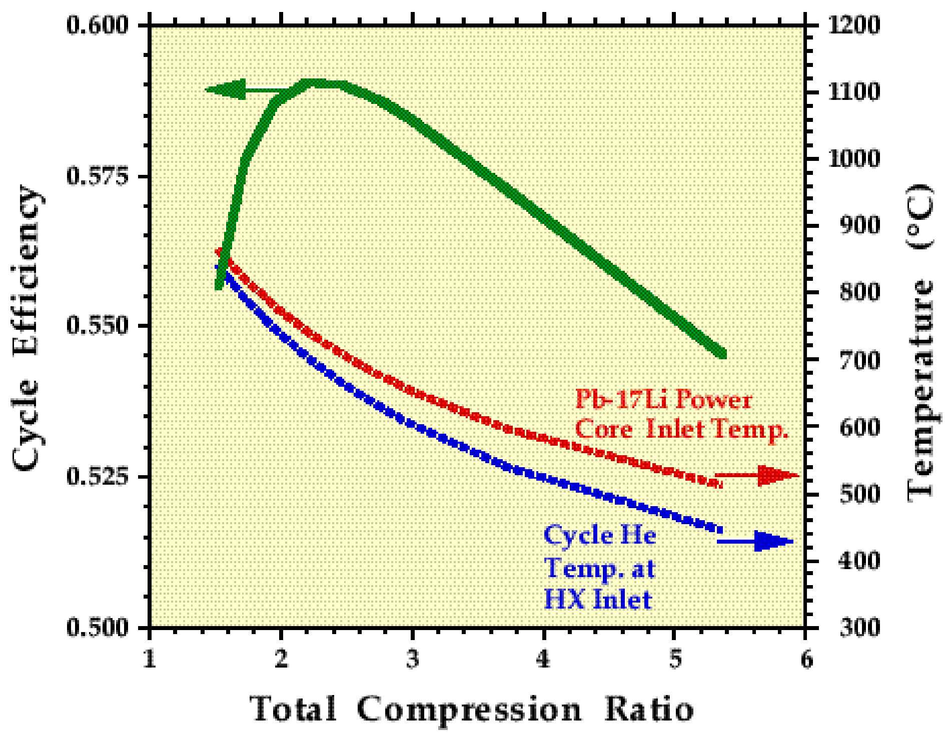

0.600
0.575
0.550
0.525
0.500
Cycle Efficiency
1200
1100
1000
900
800
700
600
500
400
300
Temperature (°C)
1
2
3
4
5
6
Total Compression Ratio
Pb-17Li Power
Core Inlet Temp.
Cycle He
Temp. at
HX Inlet

Figure 3

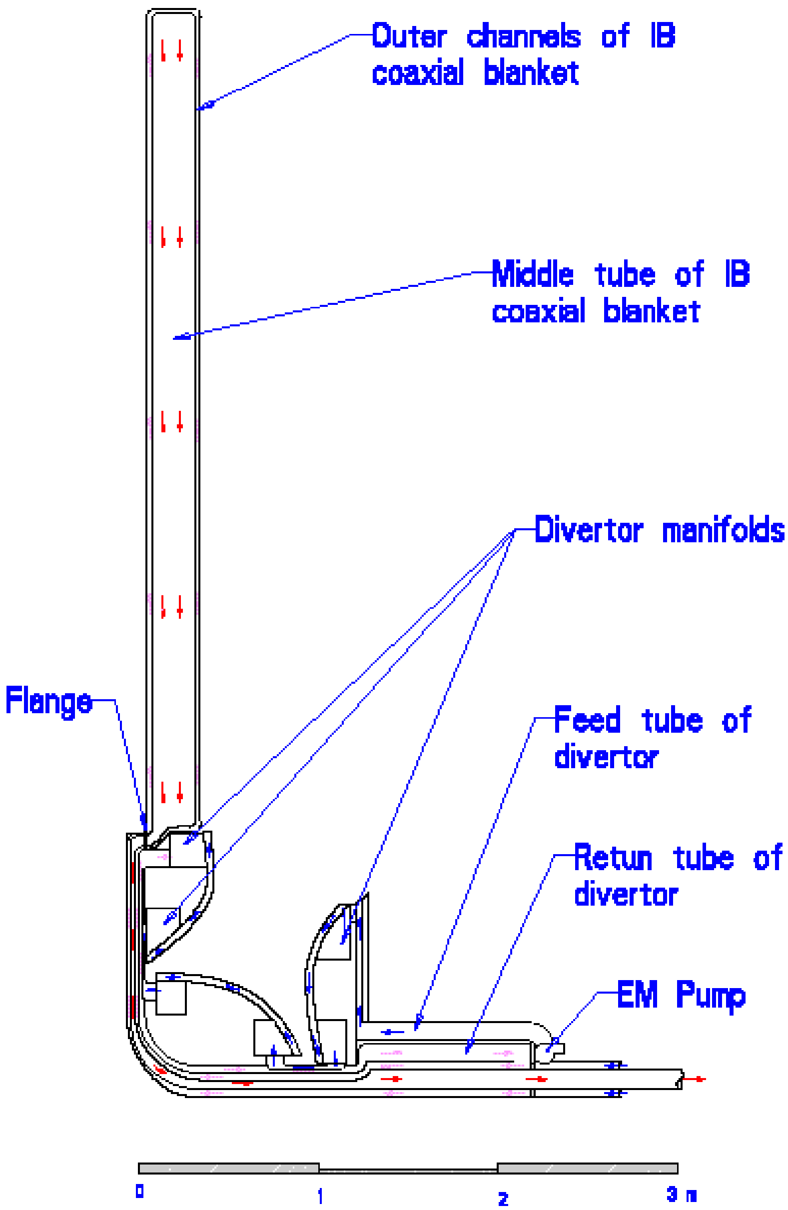
Outer channels of IB coaxial blanket
Middle tube of IB coaxial blanket
Divertor manifolds
Flange
Feed tube of divertor
Retun tube of divertor
EM Pump
0
1
2
3 m

Figure 4

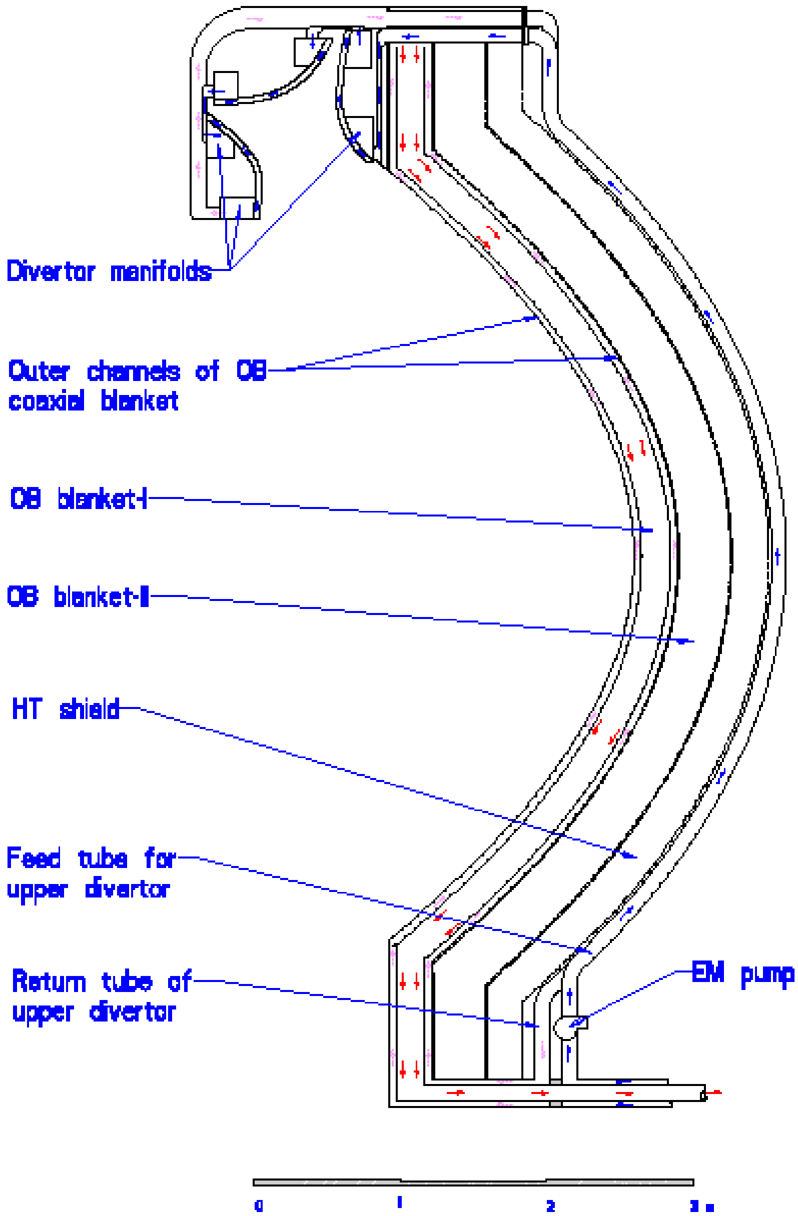
Divertor manifolds
Outer channels of OB coaxial blanket
OB blanket-I
OB blanket-II
HT shield
Feed tube for upper divertor
Return tube of upper divertor
EM pump
0
1
2
3 m

Figure 5

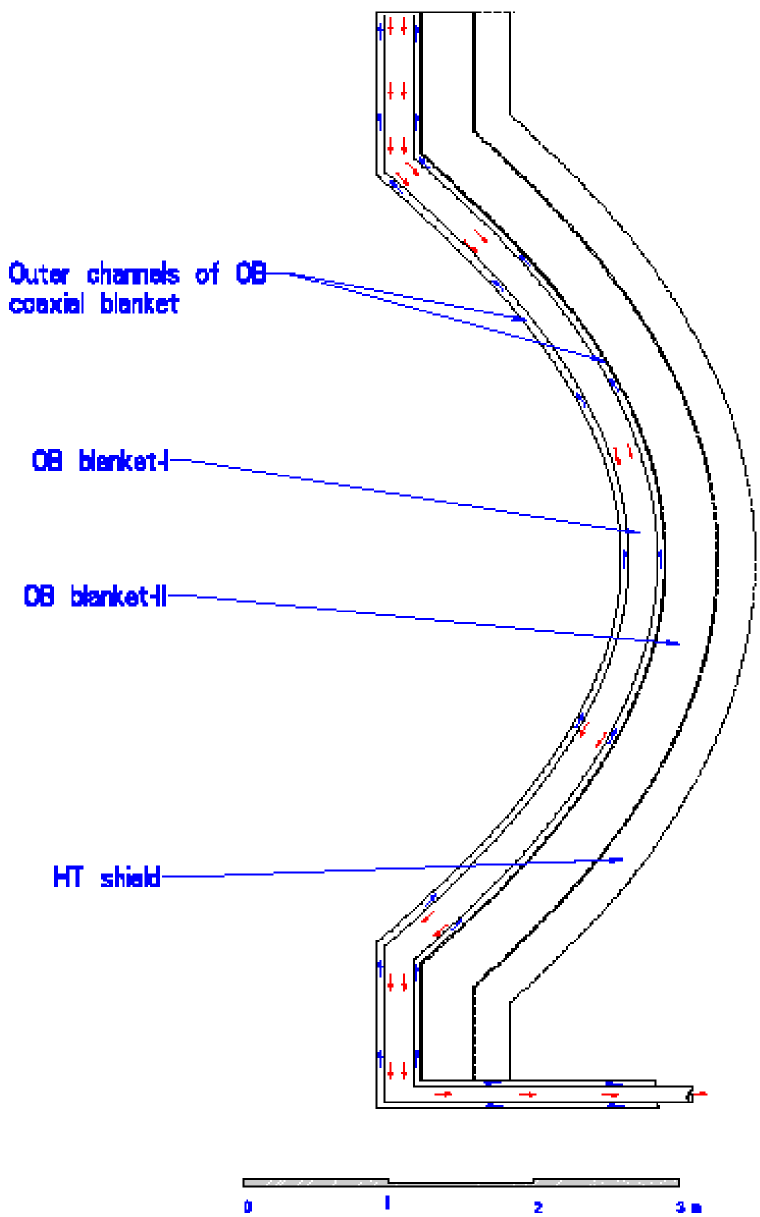
Outer channels of OB coaxial blanket
OB blanket-I
OB blanket-II
HT shield
0
1
2
3 m

Figure 6

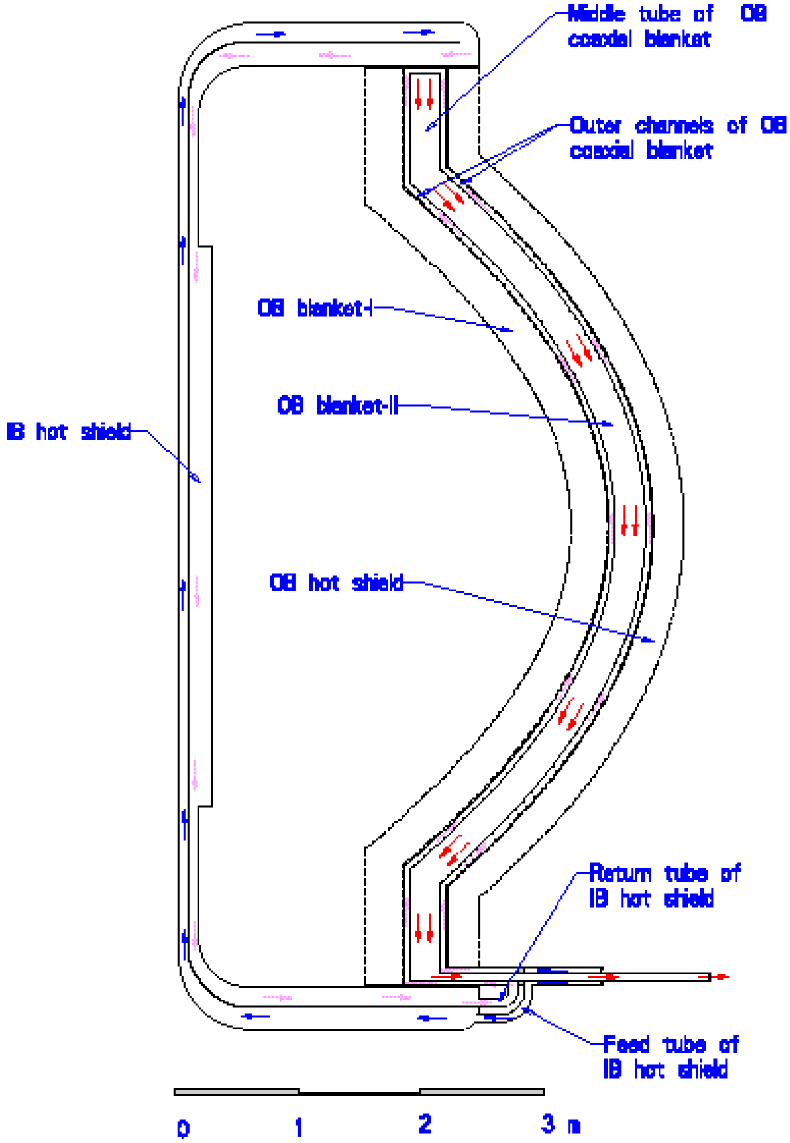
Middle tube of OB coaxial blanket
Outer channels of OB coaxial blanket
OB blanket-I
OB blanket-II
IB hot shield
OB hot shield
Return tube of IB hot shield
Feed tube of IB hot shield
0
1
2
3 m

Figure 7

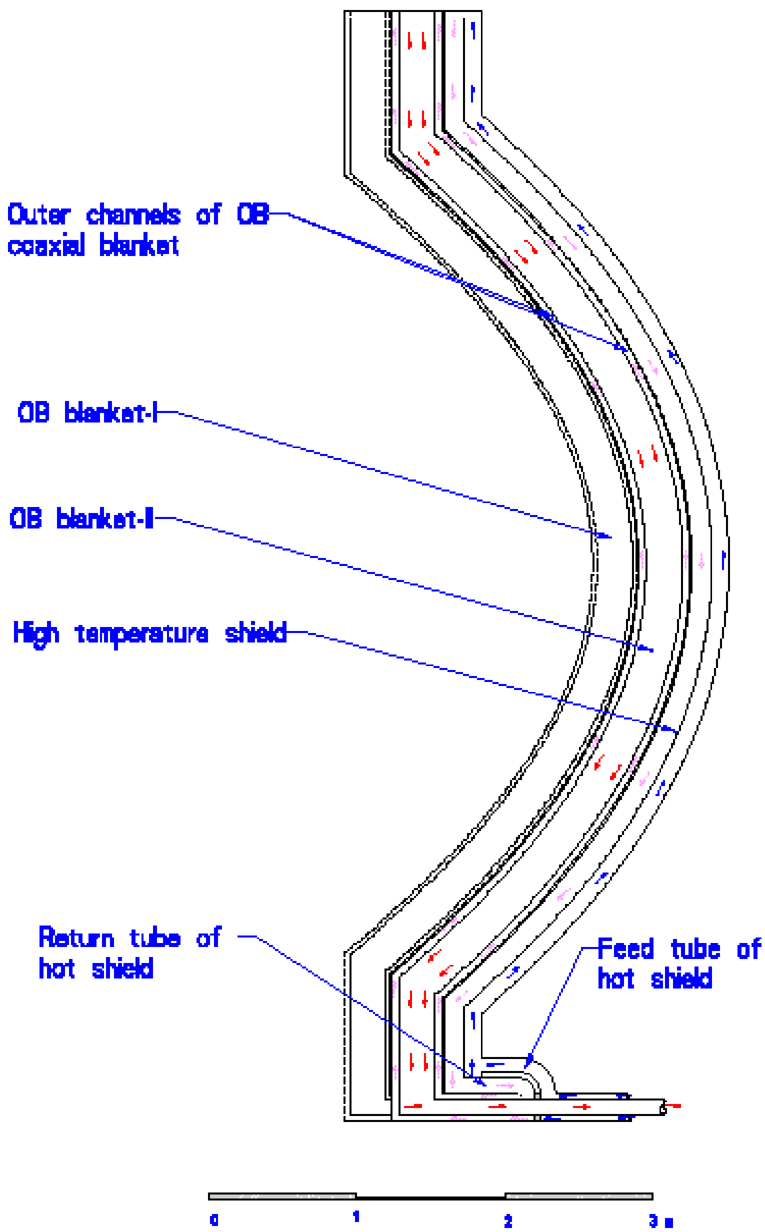

Outer channels of OB coaxial blanket
OB blanket-I
OB blanket-II
High temperature shield
Return tube of hot shield
Feed tube of hot shield
0
1
2
3 m

Figure 8

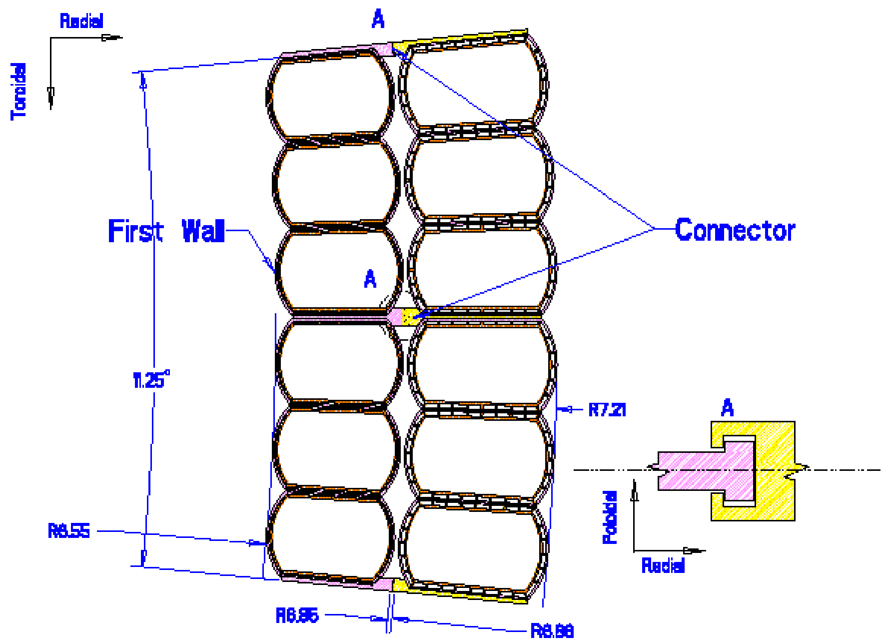

Radial
Toroidal
A
First Wall
Connector
A
11.25°
R7.21
A
Poloidal
Radial
R6.55
R6.85
R8.98

Figure 9

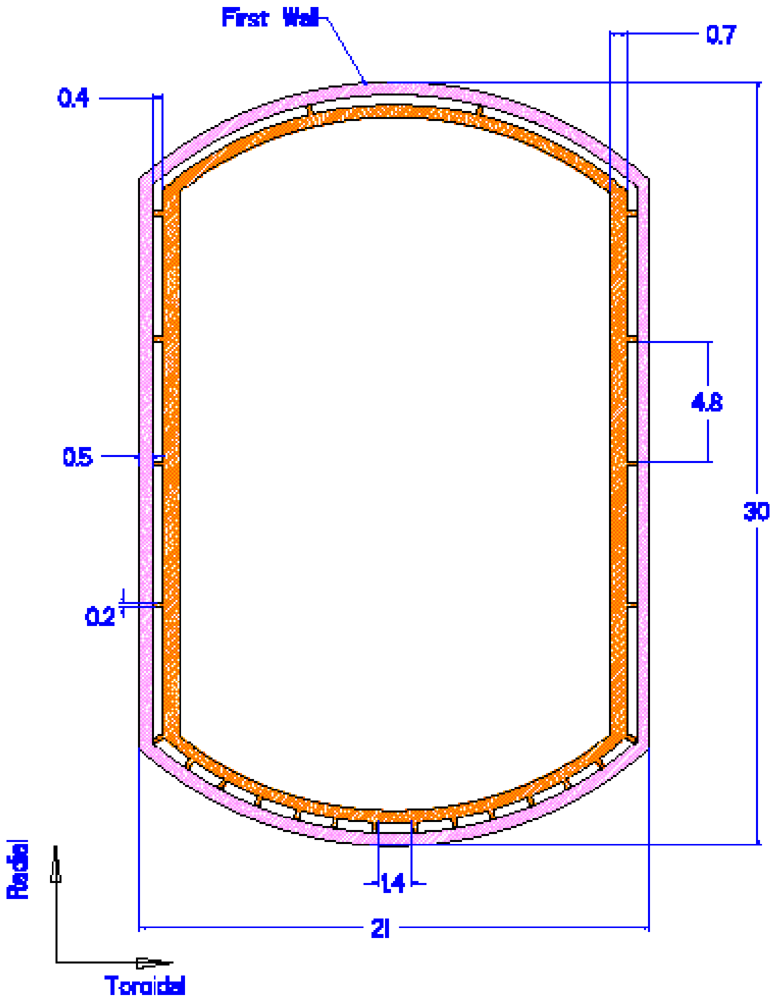

Figure 10

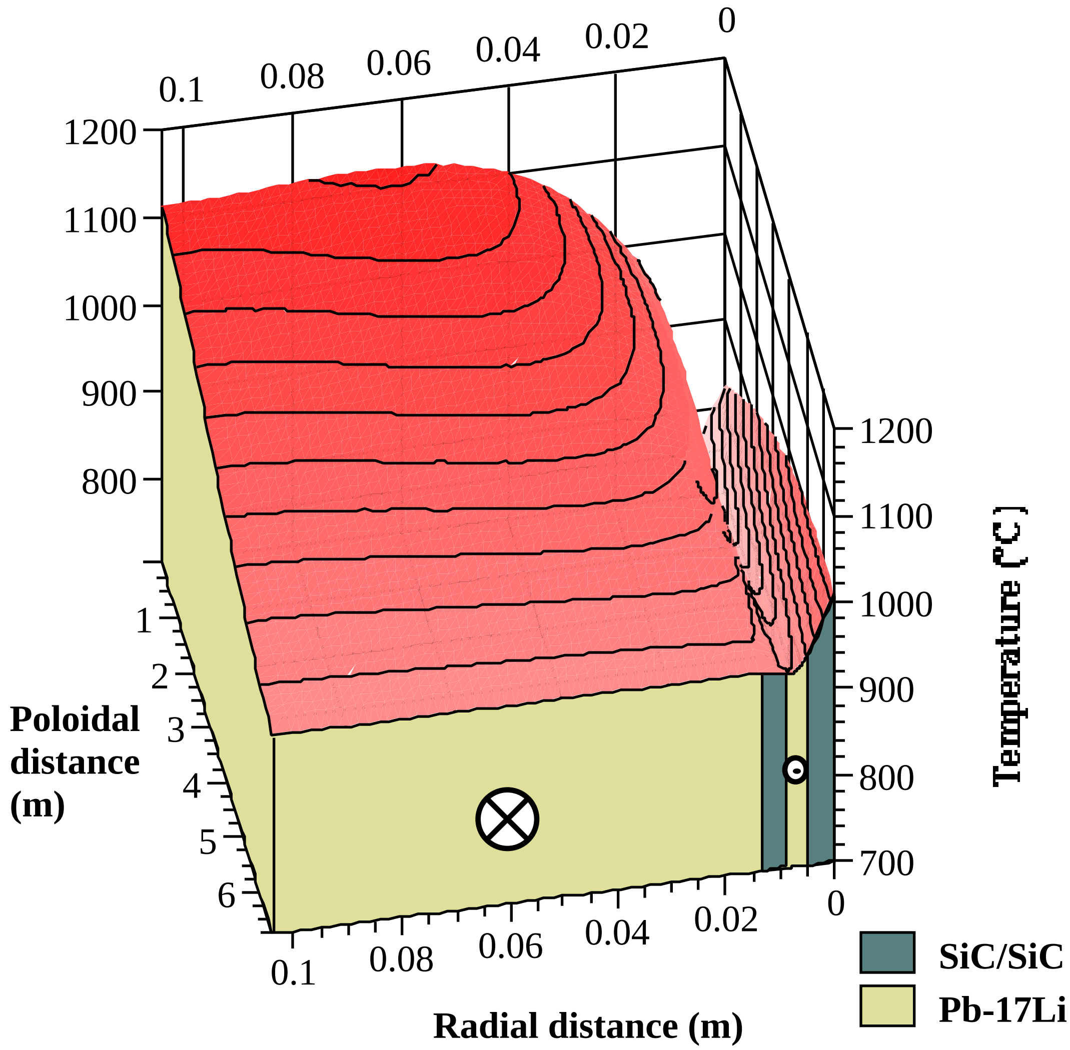

0.1
0.08
0.06
0.04
0.02
0
1200
1100
1000
900
800
1200
1100
1000
900
800
700
Temperature (°C)
1
2
3
4
5
6
Poloidal distance (m)
0.1
0.08
0.06
0.04
0.02
0
Radial distance (m)
SiC/SiC
Pb-17Li

Figure 11

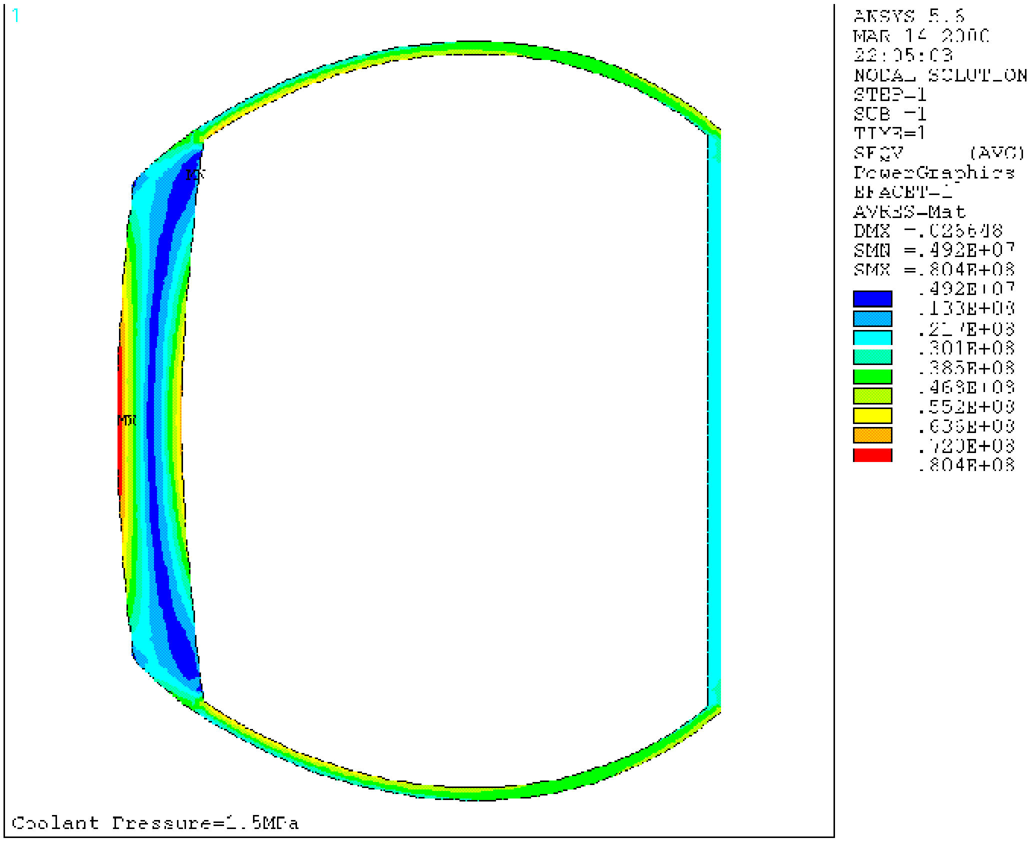
1
ANSYS 5.6
MAR 14 2000
22:05:03
NODAL SOLUTION
STEP=1
SUB =1
TIME=1
SEQV (AVG)
PowerGraphics
EFACET=1
AVRES=Mat
DMX =.025648
SMN =.492E+07
SMX =.804E+08
.492E+07
.133E+08
.217E+08
.301E+08
.385E+08
.468E+08
.552E+08
.636E+08
.720E+08
.804E+08
MN
MX
Coolant Pressure=1.5MPa

Figure 12


ANSYS 5.6
MAR 9 2000
12:20:07
NODAL SOLUTION
STEP=1
SUB =1
TIME=1
SEQV (AVG)
PowerGraphics
EFACET=1
AVRES=Mat
DMX =1.5
SMN =45079
SMX =.113E+09
45079
.126E+08
.252E+08
.378E+08
.503E+08
.629E+08
.755E+08
.881E+08
.101E+09
.113E+09
MX
MN
Outboard FW&Blanket Thermal Stress

Figure 13

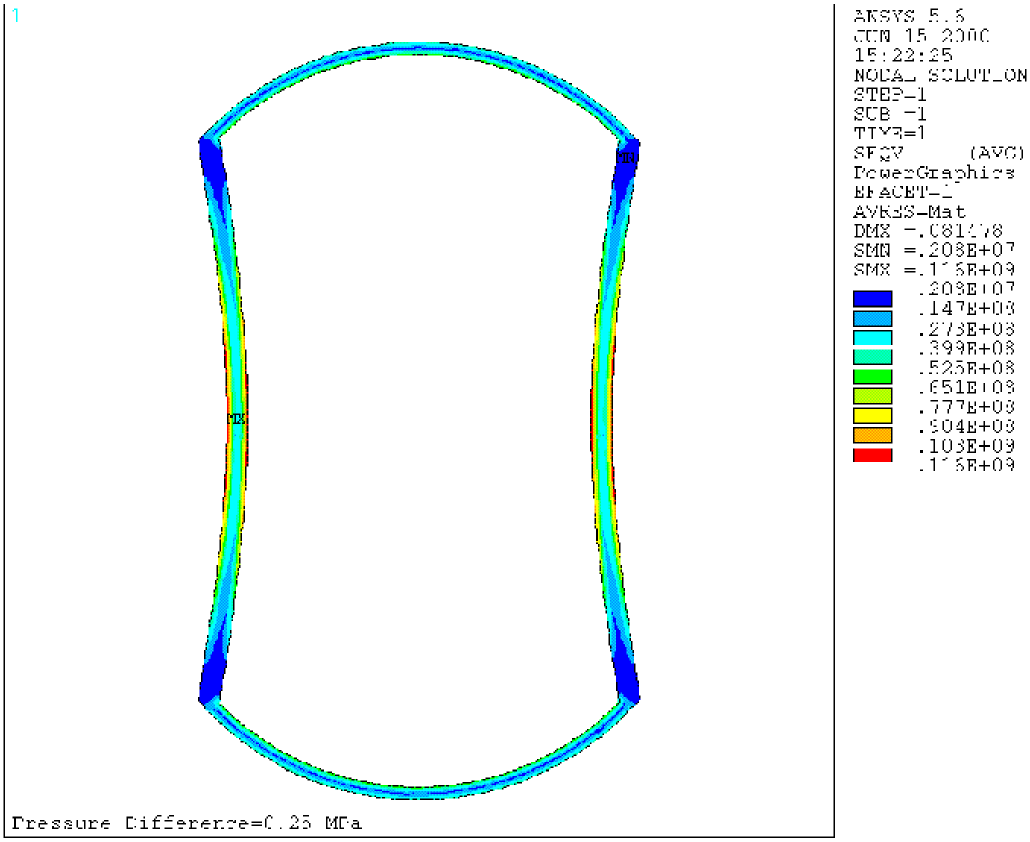
ANSYS 5.6
15:22:25
STEP=1
SUB =1
SEQV (AVG)
PowerGraphics
AVRES=Mat
SMN =.208E+07
.208E+07
.147E+08
.273E+08
.399E+08
.525E+08
.651E+08
.777E+08
.904E+08
.103E+09
Pressure Difference=0.25 MPa

Figure 14

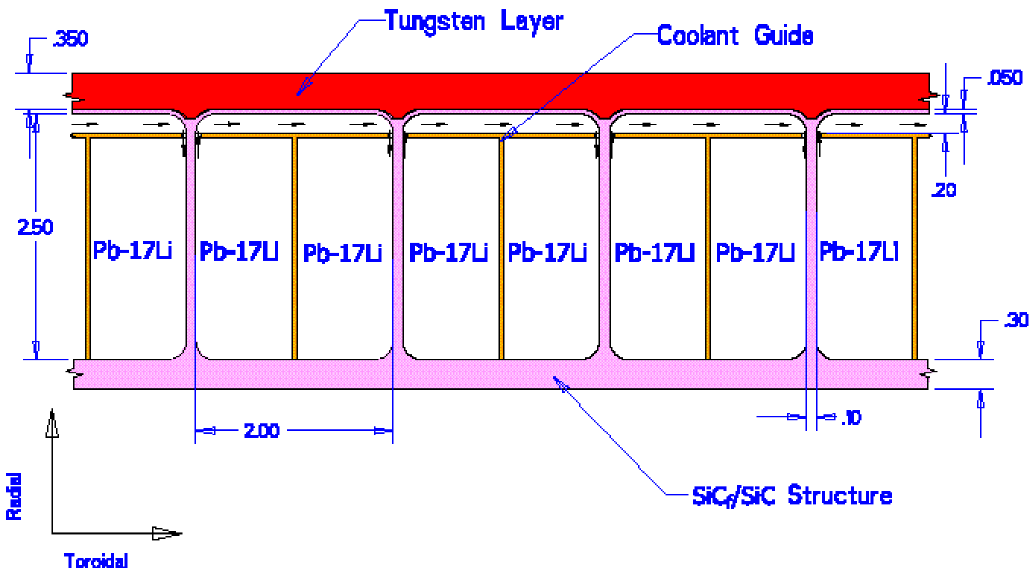

Tungsten Layer
Coolant Guide
.350
.050
.20
2.50
Pb-17Li
Pb-17Li
Pb-17Li
Pb-17Li
Pb-17Li
Pb-17Li
Pb-17Li
Pb-17Li
.30
2.00
.10
Radial
Toroidal
SiC$_f$/SiC Structure

Figure 15

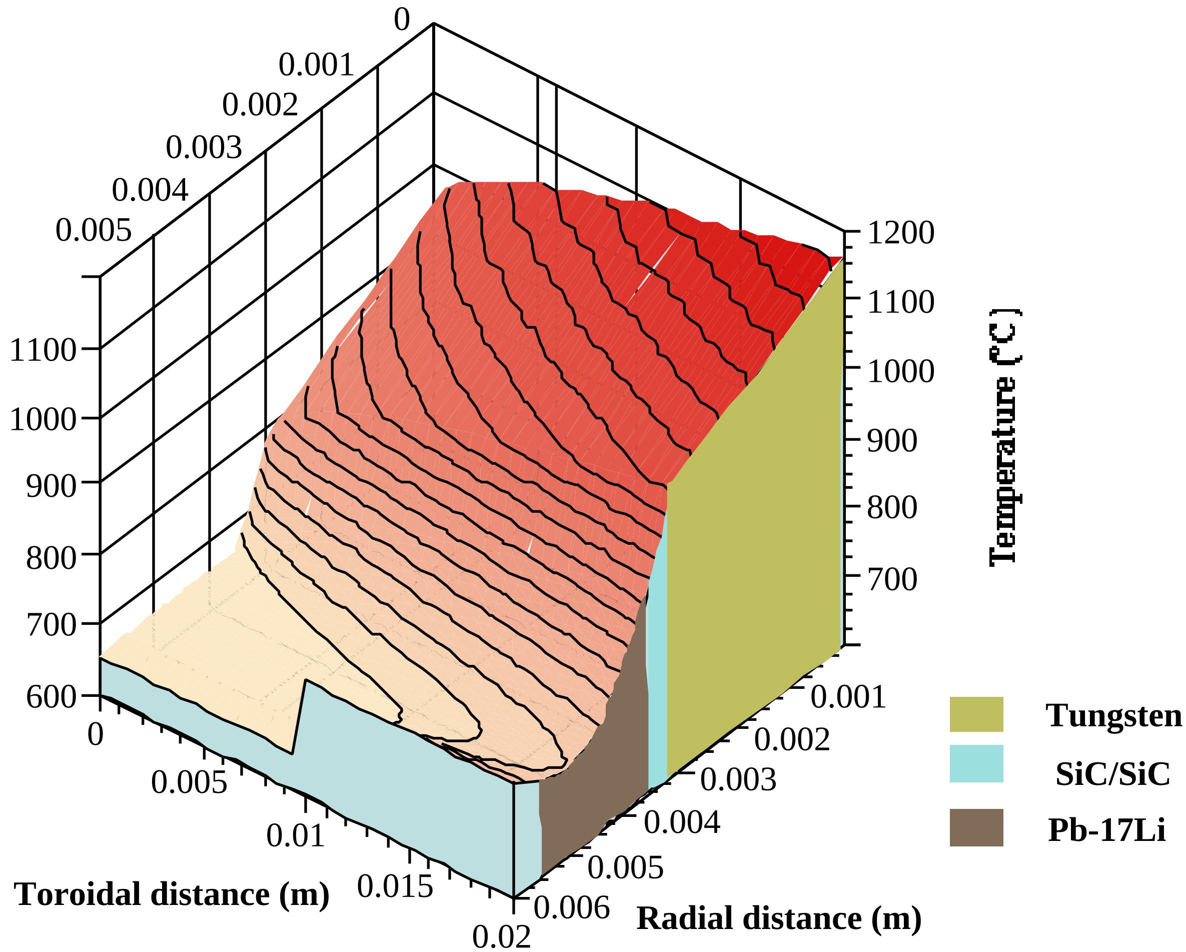

0
0.001
0.002
0.003
0.004
0.005
1100
1000
900
800
700
600
1200
1100
1000
900
800
700
Temperature (°C)
0
0.005
0.01
0.015
0.02
Toroidal distance (m)
0.001
0.002
0.003
0.004
0.005
0.006
Radial distance (m)
Tungsten
SiC/SiC
Pb-17Li

Figure 16

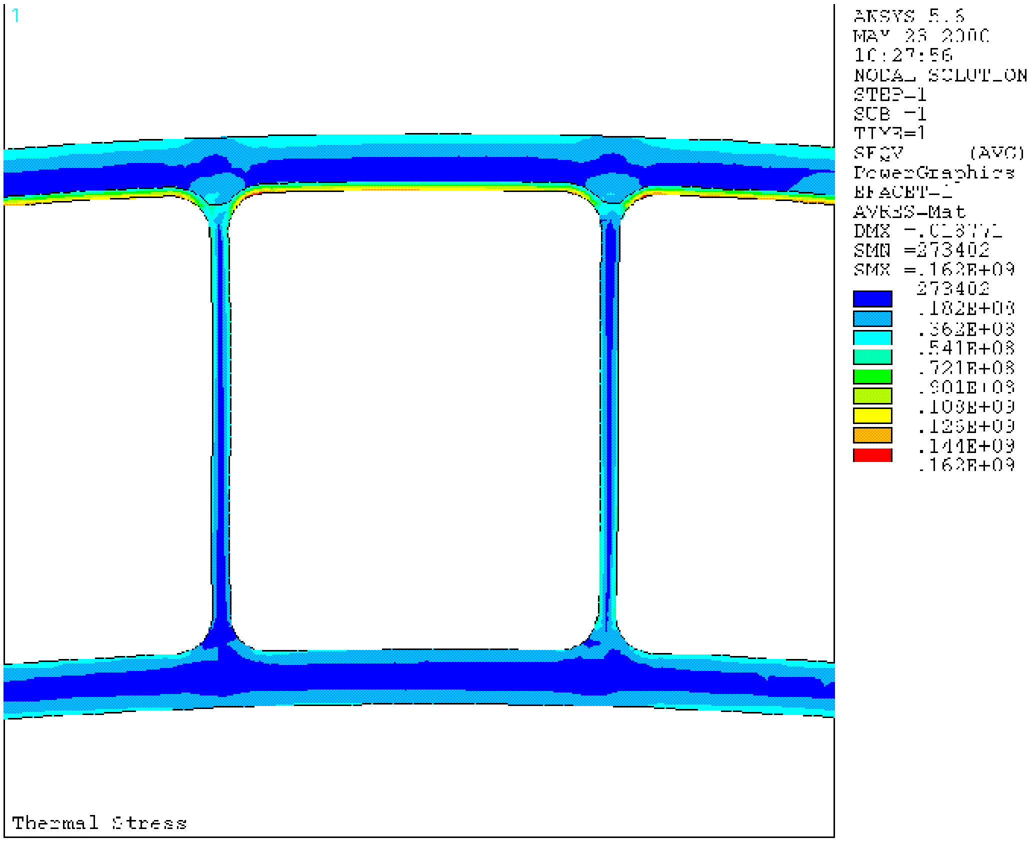
1
ANSYS 5.6
MAY 23 2000
10:27:56
NODAL SOLUTION
STEP=1
SUB =1
TIME=1
SEQV (AVG)
PowerGraphics
EFACET=1
AVRES=Mat
SMN =273402
SMX =.162E+09
273402
.182E+08
.362E+08
.541E+08
.721E+08
.901E+08
.108E+09
.126E+09
.144E+09
.162E+09
Thermal Stress

Figure 17

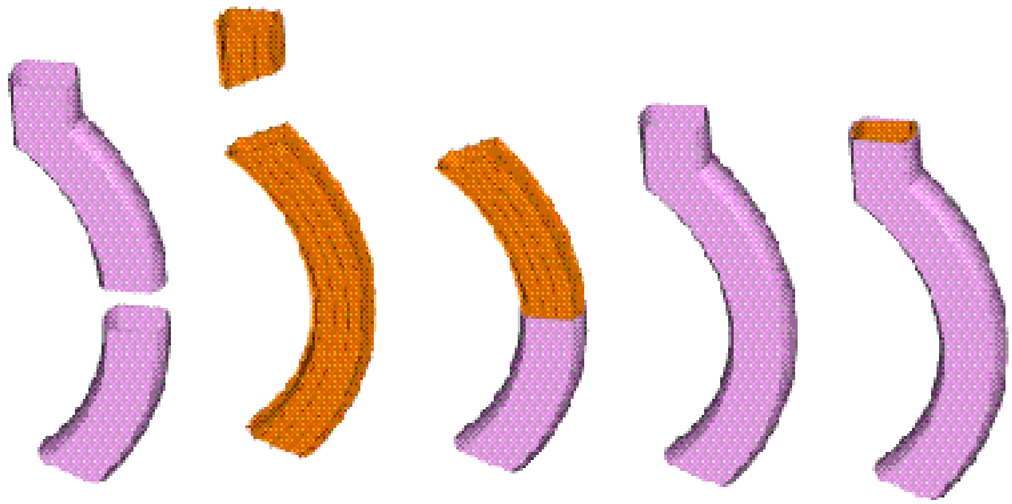

Figure 18a

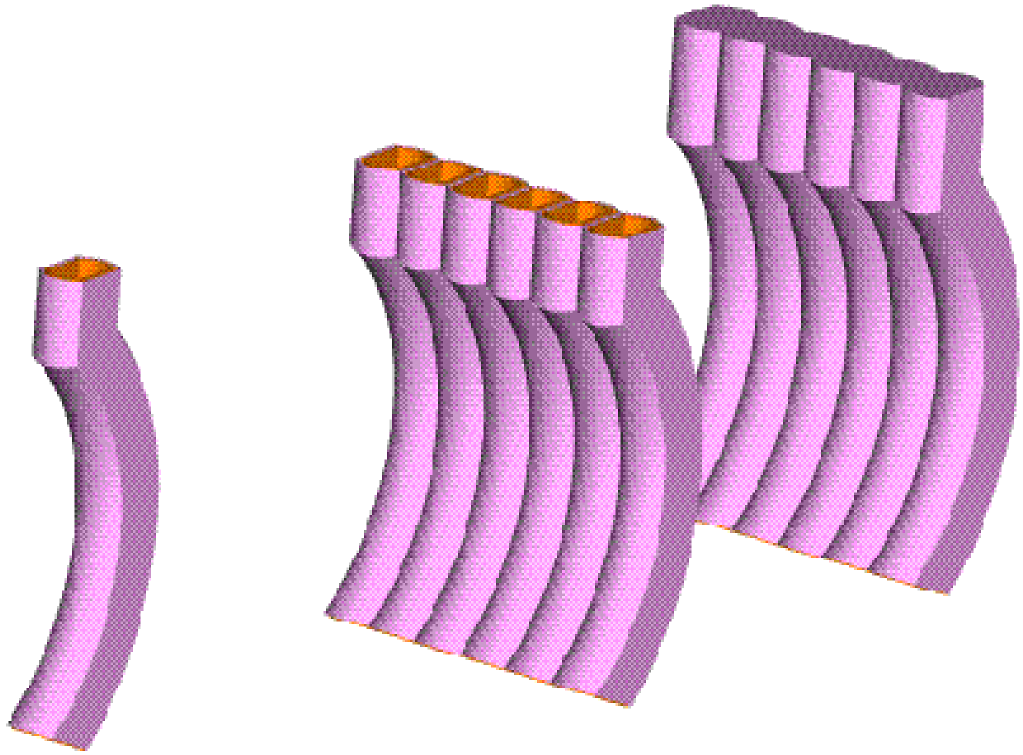

Figure 18b

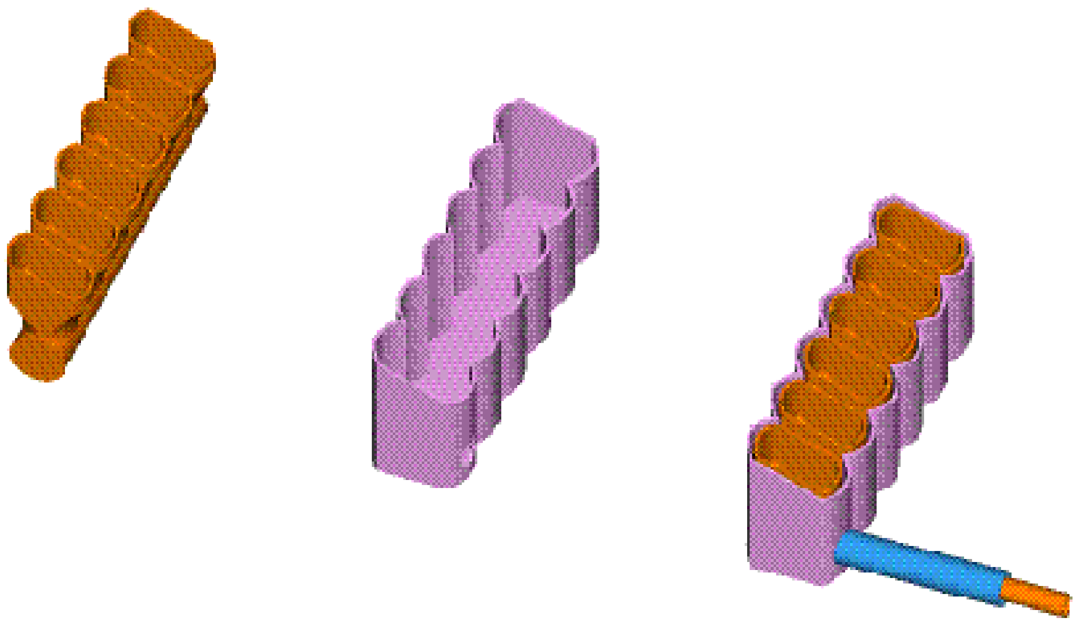

Figure 18c

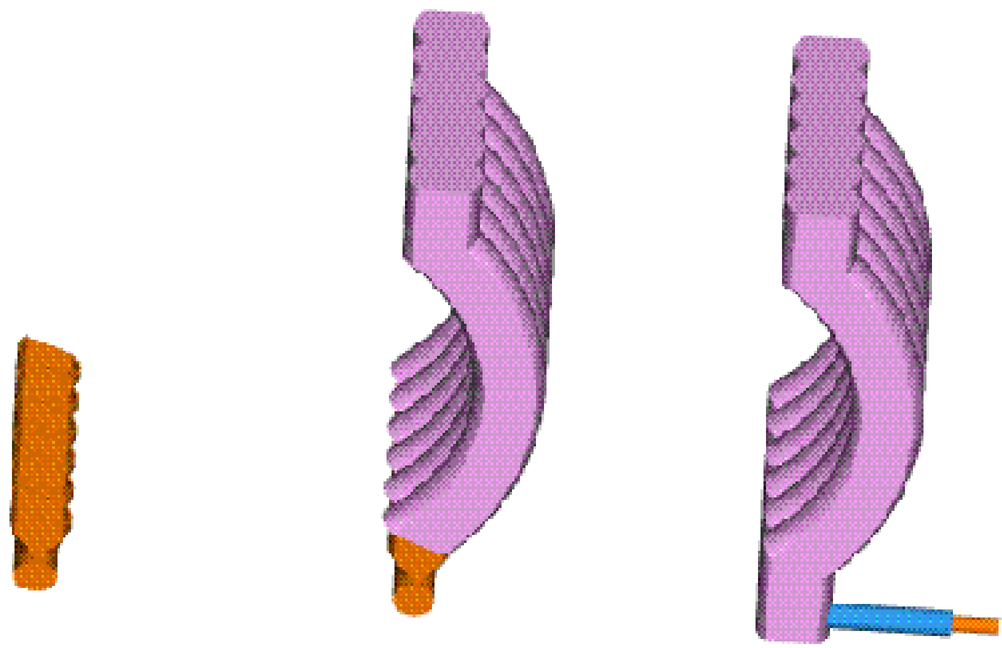

Figure 18d

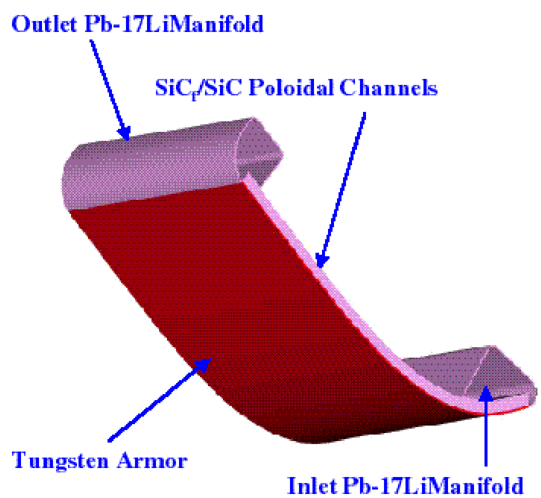
Outlet Pb-17LiManifold
SiC$_f$/SiC Poloidal Channels
Tungsten Armor
Inlet Pb-17LiManifold

Figure 19

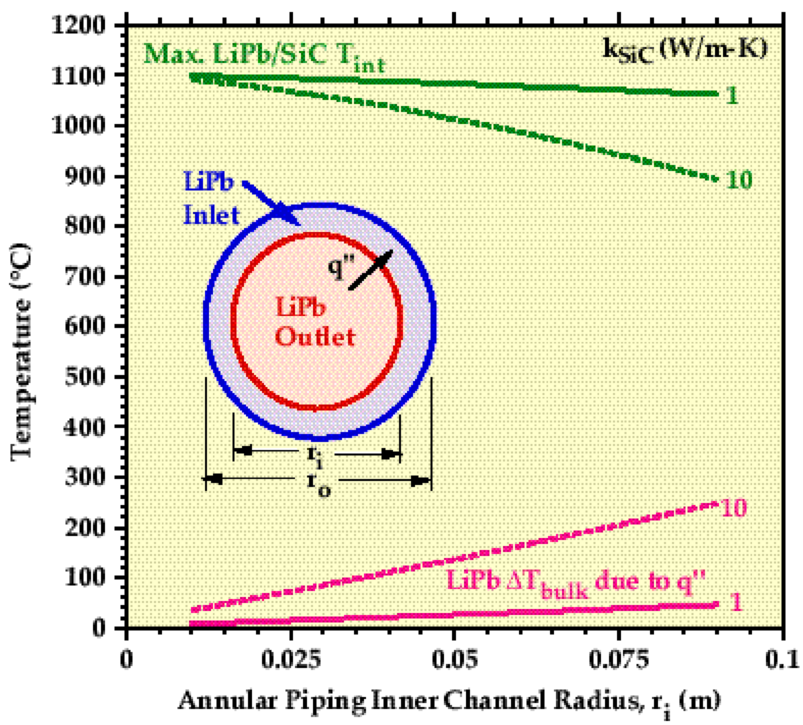

Max. LiPb/SiC T_{int}
k_{SiC} (W/m-K)
1
10
LiPb
Inlet
q"
LiPb
Outlet
r_i
r_o
10
LiPb ΔT_{bulk} due to q"
1
1200
1100
1000
900
800
700
600
500
400
300
200
100
0
Temperature (°C)
0
0.025
0.05
0.075
0.1
Annular Piping Inner Channel Radius, r_i (m)

Figure 20

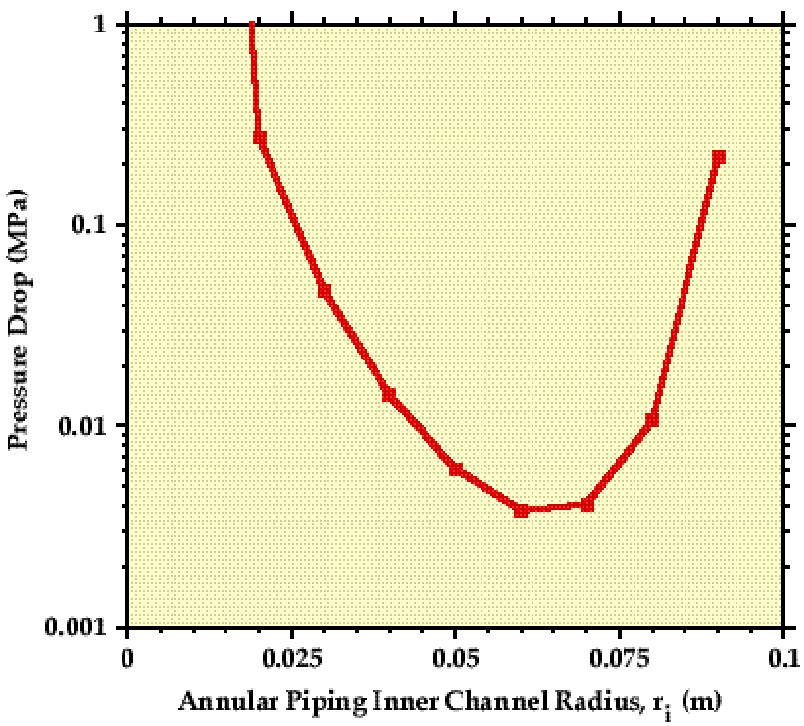

Pressure Drop (MPa)
1
0.1
0.01
0.001
0
0.025
0.05
0.075
0.1
Annular Piping Inner Channel Radius, r_i (m)

Figure 21